Measurement of the Λ_b polarization in Z decays

D. Buskulic, D. Casper, I. de Bonis, D. Decamp, P. Ghez, C. Goy, J.P. Lees, A. Lucotte, M.N. Minard, P. Odier, et al.

EUROPEAN LABORATORY FOR PARTICLE PHYSICS

CERN-PPE/95-156
November 2, 1995

Measurement of the Λ_b polarization in Z decays

The ALEPH Collaboration

Abstract

The Λ_b polarization in hadronic Z decays is measured in semileptonic decays from the average energies of the charged lepton and the neutrino. In a data sample of approximately 3 million hadronic Z decays collected by the ALEPH detector at LEP between 1991 and 1994, 462 ± 31 Λ_b candidates are selected using $(\Lambda\pi^+)$–lepton correlations. From this event sample, the Λ_b polarization is measured to be

$$\mathcal{P}_{\Lambda_b} = -0.23^{+0.24}_{-0.20}(\text{stat.})^{+0.08}_{-0.07}(\text{syst.}) \, .$$

(To be submitted to Physics Letters B)

The ALEPH Collaboration

D. Buskulic, D. Casper, I. De Bonis, D. Decamp, P. Ghez, C. Goy, J.-P. Lees, A. Lucotte, M.-N. Minard, P. Odier, B. Pietrzyk

Laboratoire de Physique des Particules (LAPP), IN^{2}P^3-CNRS, 74019 Annecy-le-Vieux Cedex, France

M. Chmeissani, J.M. Crespo, I. Efthymiopoulos, E. Fernandez, M. Fernandez-Bosman, Ll. Garrido,[15] A. Juste, M. Martinez, S. Orteu, A. Pacheco, C. Padilla, F. Palla, A. Pascual, J.A. Perlas, I. Riu, F. Sanchez, F. Teubert

Institut de Fisica d'Altes Energies, Universitat Autonoma de Barcelona, 08193 Bellaterra (Barcelona), Spain[7]

A. Colaleo, D. Creanza, M. de Palma, A. Farilla, G. Gelao, M. Girone, G. Iaselli, G. Maggi,[3] M. Maggi, N. Marinelli, S. Natali, S. Nuzzo, A. Ranieri, G. Raso, F. Romano, F. Ruggieri, G. Selvaggi, L. Silvestris, P. Tempesta, G. Zito

Dipartimento di Fisica, INFN Sezione di Bari, 70126 Bari, Italy

X. Huang, J. Lin, Q. Ouyang, T. Wang, Y. Xie, R. Xu, S. Xue, J. Zhang, L. Zhang, W. Zhao

Institute of High-Energy Physics, Academia Sinica, Beijing, The People's Republic of China[8]

R. Alemany, A.O. Bazarko, G. Bonvicini,[23] M. Cattaneo, P. Comas, P. Coyle, H. Drevermann, R.W. Forty, M. Frank, R. Hagelberg, J. Harvey, R. Jacobsen,[24] P. Janot, B. Jost, E. Kneringer, J. Knobloch, I. Lehraus, E.B. Martin, P. Mato, A. Minten, R. Miquel, Ll.M. Mir,[31] L. Moneta, T. Oest, P. Palazzi, J.R. Pater,[27] J.-F. Pusztaszeri, F. Ranjard, P. Rensing, L. Rolandi, D. Schlatter, M. Schmelling, O. Schneider, W. Tejessy, I.R. Tomalin, A. Venturi, H. Wachsmuth, T. Wildish, W. Witzeling, J. Wotschack

European Laboratory for Particle Physics (CERN), 1211 Geneva 23, Switzerland

Z. Ajaltouni, M. Bardadin-Otwinowska,[2] A. Barres, C. Boyer, A. Falvard, P. Gay, C. Guicheney, P. Henrard, J. Jousset, B. Michel, S. Monteil, J-C. Montret, D. Pallin, P. Perret, F. Podlyski, J. Proriol, J.-M. Rossignol, F. Saadi

Laboratoire de Physique Corpusculaire, Université Blaise Pascal, IN^{2}P^3-CNRS, Clermont-Ferrand, 63177 Aubière, France

T. Fearnley, J.B. Hansen, J.D. Hansen, J.R. Hansen, P.H. Hansen, B.S. Nilsson

Niels Bohr Institute, 2100 Copenhagen, Denmark[9]

A. Kyriakis, C. Markou, E. Simopoulou, I. Siotis, A. Vayaki, K. Zachariadou

Nuclear Research Center Demokritos (NRCD), Athens, Greece

A. Blondel,[21] G. Bonneaud, J.C. Brient, P. Bourdon, A. Rougé, M. Rumpf, R. Tanaka, A. Valassi,[6] M. Verderi, H. Videau[21]

Laboratoire de Physique Nucléaire et des Hautes Energies, Ecole Polytechnique, IN^{2}P^3-CNRS, 91128 Palaiseau Cedex, France

D.J. Candlin, M.I. Parsons

Department of Physics, University of Edinburgh, Edinburgh EH9 3JZ, United Kingdom[10]

E. Focardi, G. Parrini

Dipartimento di Fisica, Università di Firenze, INFN Sezione di Firenze, 50125 Firenze, Italy

M. Corden, M. Delfino,[12] C. Georgiopoulos, D.E. Jaffe

Supercomputer Computations Research Institute, Florida State University, Tallahassee, FL 32306-4052, USA [13,14]

A. Antonelli, G. Bencivenni, G. Bologna,[4] F. Bossi, P. Campana, G. Capon, V. Chiarella, G. Felici, P. Laurelli, G. Mannocchi,[5] F. Murtas, G.P. Murtas, L. Passalacqua, M. Pepe-Altarelli

Laboratori Nazionali dell'INFN (LNF-INFN), 00044 Frascati, Italy

L. Curtis, S.J. Dorris, A.W. Halley, I.G. Knowles, J.G. Lynch, V. O'Shea, C. Raine, P. Reeves, J.M. Scarr, K. Smith, A.S. Thompson, F. Thomson, S. Thorn, R.M. Turnbull

Department of Physics and Astronomy, University of Glasgow, Glasgow G12 8QQ,United Kingdom[10]

U. Becker, O. Braun, C. Geweniger, G. Graefe, P. Hanke, V. Hepp, E.E. Kluge, A. Putzer, B. Rensch, M. Schmidt, J. Sommer, H. Stenzel, K. Tittel, S. Werner, M. Wunsch

Institut für Hochenergiephysik, Universität Heidelberg, 69120 Heidelberg, Fed. Rep. of Germany[16]

D. Abbaneo, R. Beuselinck, D.M. Binnie, W. Cameron, D.J. Colling, P.J. Dornan, N. Konstantinidis, A. Moutoussi, J. Nash, G. San Martin, J.K. Sedgbeer, A.M. Stacey

Department of Physics, Imperial College, London SW7 2BZ, United Kingdom[10]

G. Dissertori, P. Girtler, D. Kuhn, G. Rudolph

Institut für Experimentalphysik, Universität Innsbruck, 6020 Innsbruck, Austria[18]

C.K. Bowdery, T.J. Brodbeck, P. Colrain, G. Crawford, A.J. Finch, F. Foster, G. Hughes, T. Sloan, E.P. Whelan, M.I. Williams

Department of Physics, University of Lancaster, Lancaster LA1 4YB, United Kingdom[10]

A. Galla, A.M. Greene, K. Kleinknecht, G. Quast, J. Raab, B. Renk, H.-G. Sander, R. Wanke, P. van Gemmeren C. Zeitnitz

Institut für Physik, Universität Mainz, 55099 Mainz, Fed. Rep. of Germany[16]

J.J. Aubert,[21] A.M. Bencheikh, C. Benchouk, A. Bonissent,[21] G. Bujosa, D. Calvet, J. Carr, C. Diaconu, F. Etienne, M. Thulasidas, D. Nicod, P. Payre, D. Rousseau, M. Talby

Centre de Physique des Particules, Faculté des Sciences de Luminy, IN^{2}P^3-CNRS, 13288 Marseille, France

I. Abt, R. Assmann, C. Bauer, W. Blum, D. Brown,[24] H. Dietl, F. Dydak,[21] G. Ganis, C. Gotzhein, K. Jakobs, H. Kroha, G. Lütjens, G. Lutz, W. Männer, H.-G. Moser, R. Richter, A. Rosado-Schlosser, S. Schael, R. Settles, H. Seywerd, R. St. Denis, W. Wiedenmann, G. Wolf

Max-Planck-Institut für Physik, Werner-Heisenberg-Institut, 80805 München, Fed. Rep. of Germany[16]

J. Boucrot, O. Callot, A. Cordier, F. Courault, M. Davier, L. Duflot, J.-F. Grivaz, Ph. Heusse, M. Jacquet, D.W. Kim,[19] F. Le Diberder, J. Lefrançois, A.-M. Lutz, I. Nikolic, H.J. Park, I.C. Park, M.-H. Schune, S. Simion, J.-J. Veillet, I. Videau

Laboratoire de l'Accélérateur Linéaire, Université de Paris-Sud, IN^{2}P^3-CNRS, 91405 Orsay Cedex, France

P. Azzurri, G. Bagliesi, G. Batignani, S. Bettarini, C. Bozzi, G. Calderini, M. Carpinelli, M.A. Ciocci, V. Ciulli, R. Dell'Orso, R. Fantechi, I. Ferrante, L. Foà,[1] F. Forti, A. Giassi, M.A. Giorgi, A. Gregorio, F. Ligabue, A. Lusiani, P.S. Marrocchesi, A. Messineo, G. Rizzo, G. Sanguinetti, A. Sciabà, P. Spagnolo, J. Steinberger, R. Tenchini, G. Tonelli,[26] C. Vannini, P.G. Verdini, J. Walsh

Dipartimento di Fisica dell'Università, INFN Sezione di Pisa, e Scuola Normale Superiore, 56010 Pisa, Italy

A.P. Betteridge, G.A. Blair, L.M. Bryant, F. Cerutti, J.T. Chambers, Y. Gao, M.G. Green, D.L. Johnson, T. Medcalf, P. Perrodo, J.A. Strong, J.H. von Wimmersperg-Toeller

Department of Physics, Royal Holloway & Bedford New College, University of London, Surrey TW20 OEX, United Kingdom[10]

D.R. Botterill, R.W. Clifft, T.R. Edgecock, S. Haywood, M. Edwards, P. Maley, P.R. Norton, J.C. Thompson

Particle Physics Dept., Rutherford Appleton Laboratory, Chilton, Didcot, Oxon OX11 OQX, United Kingdom[10]

B. Bloch-Devaux, P. Colas, S. Emery, W. Kozanecki, E. Lançon, M.C. Lemaire, E. Locci, B. Marx, P. Perez, J. Rander, J.-F. Renardy, A. Roussarie, J.-P. Schuller, J. Schwindling, A. Trabelsi, B. Vallage

CEA, DAPNIA/Service de Physique des Particules, CE-Saclay, 91191 Gif-sur-Yvette Cedex, France[17]

R.P. Johnson, H.Y. Kim, A.M. Litke, M.A. McNeil, G. Taylor

Institute for Particle Physics, University of California at Santa Cruz, Santa Cruz, CA 95064, USA[22]

A. Beddall, C.N. Booth, R. Boswell, C.A.J. Brew, S. Cartwright, F. Combley, A. Koksal, M. Letho, W.M. Newton, C. Rankin, J. Reeve, L.F. Thompson

Department of Physics, University of Sheffield, Sheffield S3 7RH, United Kingdom[10]

A. Böhrer, S. Brandt, G. Cowan, E. Feigl, C. Grupen, G. Lutters, J. Minguet-Rodriguez, F. Rivera,[25] P. Saraiva, L. Smolik, F. Stephan,

Fachbereich Physik, Universität Siegen, 57068 Siegen, Fed. Rep. of Germany[16]

M. Apollonio, L. Bosisio, R. Della Marina, G. Giannini, B. Gobbo, G. Musolino, F. Ragusa[20]

Dipartimento di Fisica, Università di Trieste e INFN Sezione di Trieste, 34127 Trieste, Italy

J. Rothberg, S. Wasserbaech

Experimental Elementary Particle Physics, University of Washington, WA 98195 Seattle, U.S.A.

S.R. Armstrong, L. Bellantoni,[30] P. Elmer, Z. Feng, D.P.S. Ferguson, Y.S. Gao, S. González, J. Grahl, T.C. Greening, J.L. Harton,[28] O.J. Hayes, H. Hu, P.A. McNamara III, J.M. Nachtman, W. Orejudos, Y.B. Pan, Y. Saadi, M. Schmitt, I.J. Scott, V. Sharma,[29] J.D. Turk, A.M. Walsh, Sau Lan Wu, X. Wu, J.M. Yamartino, M. Zheng, G. Zobernig

Department of Physics, University of Wisconsin, Madison, WI 53706, USA[11]

[1] Now at CERN, 1211 Geneva 23, Switzerland.
[2] Deceased.
[3] Now at Dipartimento di Fisica, Università di Lecce, 73100 Lecce, Italy.
[4] Also Istituto di Fisica Generale, Università di Torino, Torino, Italy.
[5] Also Istituto di Cosmo-Geofisica del C.N.R., Torino, Italy.
[6] Supported by the Commission of the European Communities, contract ERBCHBICT941234.
[7] Supported by CICYT, Spain.
[8] Supported by the National Science Foundation of China.
[9] Supported by the Danish Natural Science Research Council.
[10] Supported by the UK Particle Physics and Astronomy Research Council.
[11] Supported by the US Department of Energy, grant DE-FG0295-ER40896.
[12] On leave from Universitat Autonoma de Barcelona, Barcelona, Spain.
[13] Supported by the US Department of Energy, contract DE-FG05-92ER40742.
[14] Supported by the US Department of Energy, contract DE-FC05-85ER250000.
[15] Permanent address: Universitat de Barcelona, 08208 Barcelona, Spain.
[16] Supported by the Bundesministerium für Forschung und Technologie, Fed. Rep. of Germany.
[17] Supported by the Direction des Sciences de la Matière, C.E.A.
[18] Supported by Fonds zur Förderung der wissenschaftlichen Forschung, Austria.
[19] Permanent address: Kangnung National University, Kangnung, Korea.
[20] Now at Dipartimento di Fisica, Università di Milano, Milano, Italy.
[21] Also at CERN, 1211 Geneva 23, Switzerland.
[22] Supported by the US Department of Energy, grant DE-FG03-92ER40689.
[23] Now at Wayne State University, Detroit, MI 48202, USA.
[24] Now at Lawrence Berkeley Laboratory, Berkeley, CA 94720, USA.
[25] Partially supported by Colciencias, Colombia.
[26] Also at Istituto di Matematica e Fisica, Università di Sassari, Sassari, Italy.
[27] Now at Schuster Laboratory, University of Manchester, Manchester M13 9PL, UK.
[28] Now at Colorado State University, Fort Collins, CO 80523, USA.
[29] Now at University of California at San Diego, La Jolla, CA 92093, USA.
[30] Now at Fermi National Accelerator Laboratory, Batavia, IL 60510, USA.
[31] Supported by Dirección General de Investigación Científica y Técnica, Spain.

1 Introduction

In the standard model of electroweak interactions, quarks are produced in Z decays with high longitudinal polarization due to parity violation in the decay. At the Z peak, the longitudinal quark polarization is given by

$$\mathcal{P}_{\mathrm{q}} = \frac{-2\, v_{\mathrm{q}}\, a_{\mathrm{q}}}{v_{\mathrm{q}}^2 + a_{\mathrm{q}}^2}\,, \tag{1}$$

where v_{q} and a_{q} are the vector and axial couplings of the quarks to the Z boson, respectively.

With $\sin^2\theta_{\mathrm{W}} = 0.23$, the b quark longitudinal polarization is expected to be $\mathcal{P}_{\mathrm{b}} = -0.94$. Hard gluon emission and mass effects change the polarization by 3% [1], leaving the initial b quark polarization almost unchanged at the time of hadron formation. However, in the hadronization process, part or all of the initial b quark polarization may be lost by the final hadron state due to spin–spin forces in the b hadron.

The b mesons always cascade down to spin zero pseudoscalar states which do not retain any polarization information. In contrast, hadronization to b baryons might preserve a large fraction of the initial b quark polarization [2, 3]. In particular, the lightest b baryon state, Λ_{b}, is expected to carry the constituent b quark spin since the light quarks are arranged in a spin-0 and isospin-0 singlet in the constituent quark model. Higher mass baryonic states (Σ_{b} and Σ_{b}^*) are expected to transfer little of their polarization in their hadronic decays to $\Lambda_{\mathrm{b}}\pi$, implying that the net Λ_{b} polarization in an inclusive Λ_{b} sample is somewhat reduced. The expected value of the Λ_{b} polarization is estimated in Ref. [3]. From recent results on Λ_{b} production [4] and $\Sigma_{\mathrm{b}}^{(*)}$ production [5], the Λ_{b} polarization is expected, in the limit of totally incoherent Σ_{b} and Σ_{b}^* resonances, to retain $73\pm6\%$ of the initial b quark polarization.

A measurement of the sign of the Λ_{b} polarization would determine unambiguously the chirality of the b quark coupling to the weak charged current [6].

2 The ALEPH detector

A detailed description of the ALEPH detector and its performance can be found in Ref. [7, 8]. Charged particles are detected in the central part of the detector consisting of a precision vertex detector (VDET), a cylindrical multi-wire drift chamber (ITC) and a large time projection chamber (TPC). Surrounding the beam pipe, the VDET consists of two concentric layers of double-sided silicon detectors, positioned at average radii of 6.5 cm and 11.3 cm, and covering respectively 85% and 69% of the solid angle. The intrinsic spatial resolution of the VDET is 12 μm for the $r\phi$ coordinate and between 11 μm and 22 μm for the z coordinate, depending on the polar angle of the charged particle. The ITC, at radii between 16 cm and 26 cm, provides up to 8 coordinates per track in the $r\phi$ view while the TPC measures up to 21 three-dimensional points per track at radii between 30 cm and 180 cm. It also serves to separate charged particle species with up to 338 measurements of the specific ionization ($\mathrm{d}E/\mathrm{d}x$). The three detectors are immersed in an axial

magnetic field of 1.5 T and together provide a transverse momentum resolution of $\sigma(1/p_T) = 0.6 \times 10^{-3}$ $(\mathrm{GeV}/c)^{-1}$.

Electrons and photons are identified in the electromagnetic calorimeter (ECAL), a lead-proportional chamber sandwich segmented into 15 mrad $\times$ 15 mrad projective towers which are read out in three sections in depth. Muons are identified in the hadron calorimeter (HCAL), a seven interaction length yoke interleaved with 23 layers of streamer tubes, together with two additional double layers of muon chambers.

The total visible energy in the detector is determined with an energy flow algorithm [8] which combines measurements from different detector components, to achieve a relative precision of $0.60/\sqrt{E/\mathrm{GeV}}$. This algorithm is used in the present analysis to compute the missing energy in the b hadron hemisphere.

3 Λ_b selection and analysis procedure

The fraction of initial b quark polarization that survives hadronization to a Λ_b is studied using the inclusive semileptonic decay $\Lambda_b \to X_c\, \ell^- \bar{\nu}_\ell$, where X_c is any charmed hadron state. This decay channel is copiously produced and can be tagged using the charge correlation between the lepton and a $\Lambda\pi^+$ combination which is frequently present in the cascade decay of the charmed hadron.

To evaluate the Λ_b polarization from inclusive Λ_b semileptonic decays, the method of Ref. [9] is adopted which consists of measuring the ratio of the average energy of the lepton to that of the neutrino, $y = \langle E_\ell \rangle / \langle E_\nu \rangle$. This ratio y has a simple and large dependence on the Λ_b polarization $\mathcal{P}_{\Lambda_b}$:

$$y = \frac{\langle E_\ell \rangle}{\langle E_\nu \rangle} = \frac{7 - \mathcal{P}_{\Lambda_b}}{6 + 2\mathcal{P}_{\Lambda_b}} + \mathcal{O}(m_c^2/m_b^2)\,. \tag{2}$$

The uncertainty on the term $\mathcal{O}(m_c^2/m_b^2)$ induces an error on $\mathcal{P}_{\Lambda_b}$ of a few percent.

This method is more sensitive to Λ_b polarization than other proposed methods[10] for the following reasons.

- In the inclusive limit, the energy and the angular distributions of the lepton and the neutrino differ from those from free quark decay, $b \to c\, \ell^- \bar{\nu}_\ell$, only to order $(\Lambda_{QCD}/m_b)^2 \approx 1\%$ [11]. The major theoretical uncertainty in the description of the decay is due to the unknown quark masses. Exclusive methods, on the contrary, suffer from large theoretical uncertainties associated to poorly known form factors.

- The lepton average energy is, up to m_c^2/m_b^2 terms, proportional to $7 - \mathcal{P}_{\Lambda_b}$, and increases with increasing left–handedness. The neutrino average energy is, up to ϵ terms, proportional to $6 + 2\mathcal{P}_{\Lambda_b}$ and decrease with increasing left–handedness. If the correlation between the charged lepton and neutrino energies is taken into account, their ratio is statistically four times more sensitive than the lepton energy alone.

- The Λ_b boost cancels out exactly in the ratio of energies. Hence this ratio is independent of hadronization effects and modelling.
- The uncertainty in the energy scale associated with the unknown mass of the recoiling charm system cancels in the ratio, with the exception of the $\mathcal{O}(m_c^2/m_b^2)$ term.

This analysis has therefore theoretical errors of a few percent and good statistical sensitivity.

3.1 Λ_b selection

This analysis is based on a sample of 2,988,819 hadronic Z decays recorded with the ALEPH detector from 1991 to 1994, selected as described in Ref. [12]. Semileptonic Λ_b decay candidates are selected using the charge correlation between a $\Lambda\pi^+$ system and a lepton in the same hemisphere. The requirement of the additional π^+ expected in the dominant $\Lambda_b \to \Lambda_c \to \Lambda X^+$ decay provides a better signal-to-noise ratio in the sample. Throughout this letter, "lepton" refers to either electron or muon, and charge conjugate reactions are implied.

Events are divided in two hemispheres by the plane perpendicular to the thrust axis. For a reliable measurement of the missing energy it is important to have well contained events in the detector. Each event is required to have $|\cos\theta_{\rm thrust}| < 0.85$, where $\theta_{\rm thrust}$ is the polar angle of the thrust axis.

Λ candidates are reconstructed, in the channel $\Lambda \to {\rm p}\pi^-$, with an algorithm which fits two oppositely charged particle tracks to a common vertex [8]. To reduce the combinatorial background, the Λ momentum is required to be in excess of 3 GeV/c and the Λ decay vertex at least 5 cm from the interaction point. Photon conversions and $\rm K^0_S$ candidates are rejected as described in Ref. [13]. The ${\rm d}E/{\rm d}x$ measurements for the two Λ daughter tracks are required, when available, to be within three standard deviations of those expected for a proton and a pion. The selected Λ candidates are then combined with pions with momentum higher than 0.2 GeV/c. Since events with a Λ_c^+ semileptonic decay may contribute to the missing energy in the $\Lambda\pi^+$ hemisphere, it is required that the pion candidate be not identified as a lepton. The invariant mass of the $\Lambda\pi^+$ system is required to be less than 2.35 GeV/c^2 and the χ^2 probability of the $\Lambda\pi^+$ vertex fit must be larger than 1%.

The selected $\Lambda\pi^+$ candidates are combined with identified leptons of momentum $p_\ell > 3$ GeV/c and transverse momentum with respect to the associated jet of $p_T > 1$ GeV/c. Finally the $(\Lambda\pi^+)\ell$ system is required to have an invariant mass less than 5.8 GeV/c^2, the χ^2 probability of the $(\Lambda\pi^+)\ell$ common vertex fit must be larger than 1%, the angle between the Λ and the lepton is required to be less than 45^o, and the cosine of the angle between the vector joining the primary vertex and the $(\Lambda\pi^+)\ell$ vertex and the $(\Lambda\pi^+)\ell$ momentum must be positive.

The resulting ${\rm p}\pi^-$ invariant mass distributions of the $(\Lambda\pi^+)\ell^-$ and the $(\Lambda\pi^+)\ell^+$ samples, hereafter called right–sign and wrong–sign samples respectively, are shown

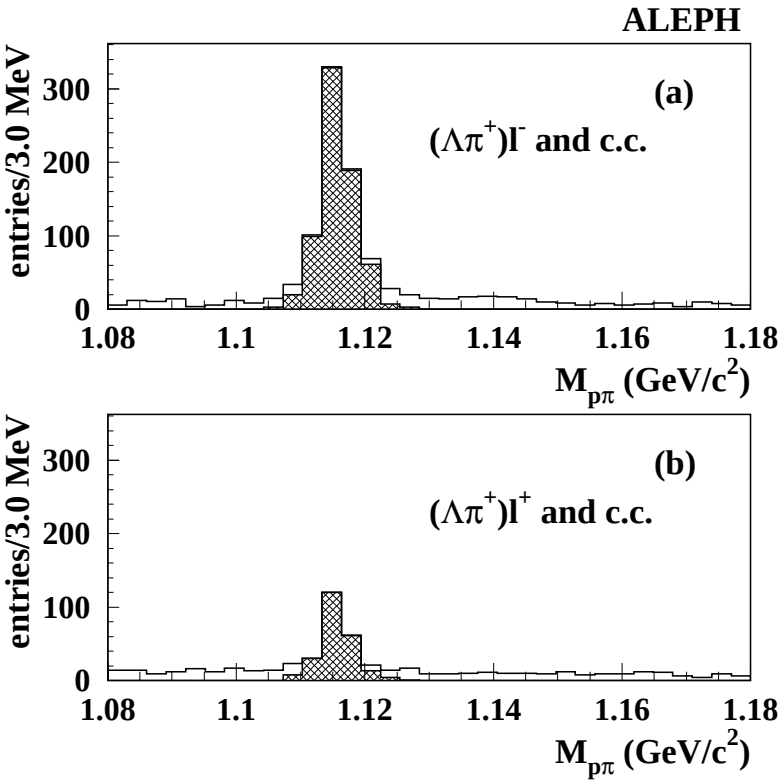

Figure 1: The $p\pi^-$ invariant mass distributions (a) for the right–sign $(\Lambda\pi^+)\ell^-$ sample and (b) the wrong–sign $(\Lambda\pi^+)\ell^+$ sample in the 1991-1994 data. The shaded areas show the selected events within the momentum dependent mass window cut (see text).

in Fig. 1. The excess of $(\Lambda\pi^+)\ell^-$ events over $(\Lambda\pi^+)\ell^+$ is attributed to Λ_b semileptonic decays. Right– and wrong–sign $(\Lambda\pi^+)\ell$ candidates are selected using a momentum dependent mass window cut of $\pm 2.5\,\sigma(p)$ around the nominal Λ mass, where $\sigma(p)$ is the Λ mass resolution at momentum p as shown by the shaded areas of Fig. 1. The excess of $(\Lambda\pi^+)\ell^-$ over $(\Lambda\pi^+)\ell^+$ events is 462 ± 31.

The right–sign sample consists of two components, *i*) the genuine signal; and *ii*) background events mainly due to accidental combinations of a real or a fake $(\Lambda\pi^+)$ in association with a real or a fake lepton. The contribution from physics background processes [13] is small. The wrong–sign sample consists mainly of accidental combinations but a small fraction of events is due to combinations between a lepton from Λ_b semileptonic decay and a Λ from fragmentation.

The selection efficiency is determined from a Monte Carlo simulation of direct and cascade Λ_b [14] subsequently decaying semileptonically and leading to a $\Lambda\pi^+$ in the hadronic decay sequence. The selection efficiency of Λ_b originating from the decay of Σ_b or Σ_b^* is expected to be $(8.22 \pm 0.15)\%$, while direct Λ_b are selected with an efficiency of $(8.78 \pm 0.16)\%$. This bias toward direct Λ_b decays tends to increase the measured Λ_b polarization by 2.5% and is neglected.

3.2 Neutrino energy measurement

The neutrino energy is measured from the missing energy in the $(\Lambda\pi^+)$ lepton hemisphere:

$$E_\nu \;=\; E_{\rm tot} - E_{\rm vis}\,, \tag{3}$$

where E_{vis} is the visible energy in the $(\Lambda\pi^+)\ell$ hemisphere, measured by the energy flow algorithm [8]. Here E_{tot} is the expected hemisphere energy, *i.e.* the beam energy corrected for the measured hemisphere masses as follows [15]:

$$E_{\rm tot} = \frac{\sqrt{s}}{2} + \frac{m^2_{\rm same} - m^2_{\rm oppo}}{2\sqrt{s}}\,. \tag{4}$$

Here $m_{\rm same}$ is the visible invariant mass of the $(\Lambda\pi^+)\ell$ hemisphere and $m_{\rm oppo}$ is the mass of the opposite hemisphere.

From Monte Carlo simulation of the $\Lambda_{\rm b}$ semileptonic decays, the neutrino energy resolution obtained with this method is $\sigma_{E_\nu} = 3.1$ GeV.

3.3 Analysis procedure and method

The selection cuts and neutrino energy reconstruction discussed above introduce a bias in the variable $y = \langle E_\ell\rangle/\langle E_\nu\rangle$. These effects can be corrected using from Monte Carlo simulation with the variable:

$$R_y^{\rm data} = \frac{y_{\rm data}}{y_{\rm MC}(0)}\,. \tag{5}$$

The value of $y_{\rm data}$ is measured from the selected data sample and the value of $y_{\rm MC}(0)$ is extracted from a fully reconstructed Monte Carlo sample of unpolarized $\Lambda_{\rm b}$ semileptonic decays using the same selection cuts. Any significant deviation of $R_y^{\rm data}$ from unity would be considered as evidence for $\Lambda_{\rm b}$ polarization. Fig. 2 shows the variation of $R_y^{\rm MC} = y_{\rm MC}(\mathcal{P}_{\Lambda_{\rm b}})/y_{\rm MC}(0)$ with $\Lambda_{\rm b}$ polarization before and after reconstruction and selection cuts. At the generator level, the theoretical prediction $R_y^{\rm th}$ (given by equation (2)) and Monte Carlo simulation agree very well. After reconstruction and selection cuts, there is a small shift which is taken into account using the parameterization

$$R_y^{\rm MC} \simeq R_y^{\rm th} - 0.06\mathcal{P}_{\Lambda_{\rm b}}\,, \tag{6}$$

obtained from Monte Carlo event samples produced with five different polarization values ($-1.$, -0.75, -0.5, -0.25, $0.$). The $R_y^{\rm data}$ value is used to extract the $\Lambda_{\rm b}$ polarization value with the $R_y^{\rm MC}$ curve.

4 Background subtraction

The charged lepton and the neutrino energy distributions of the right–sign and wrong–sign samples are shown in Fig. 3. To extract the average charged lepton energy and average neutrino energy of the genuine $\Lambda_{\rm b}$ semileptonic decays, the

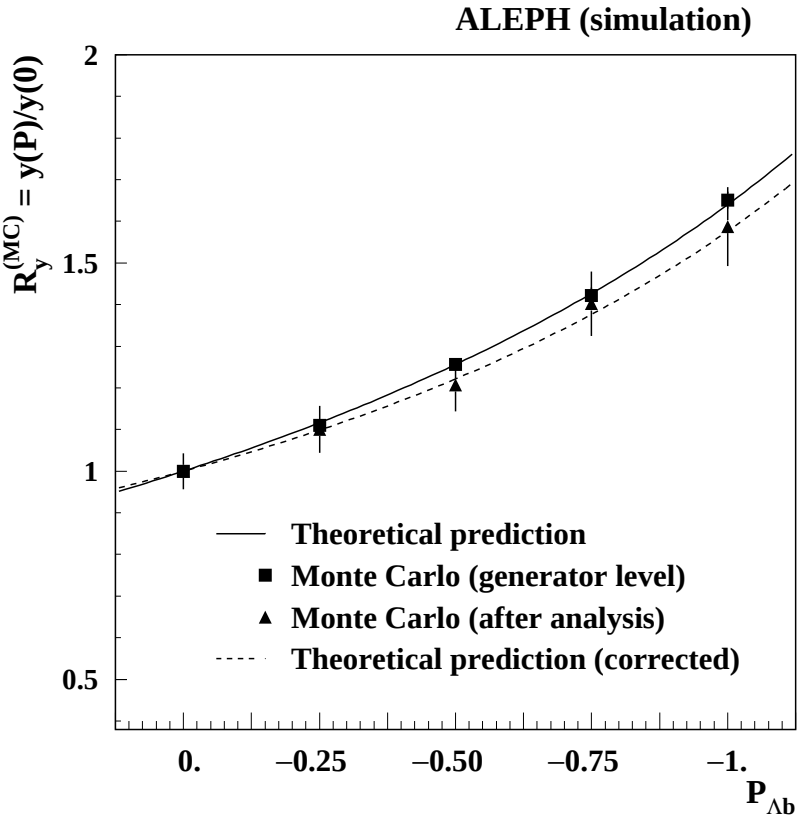

Figure 2: The variation of $R_y^{\rm MC}$ as a function of the $\Lambda_{\rm b}$ polarization. The solid curve represents the analytical expression $R_y^{\rm th}$, the squares are the simulated $R_y^{\rm MC}$ values at the generator level for different $\Lambda_{\rm b}$ polarizations, the triangles correspond to the $R_y^{\rm MC}$ values after Monte Carlo event reconstruction and selection cuts and the dashed line is the analytical expression corrected for the reconstruction and acceptance effects.

fraction and average charged lepton and neutrino energies of the background in the right–sign sample must be known. These quantities are determined from the wrong–sign sample and checked by comparing, in the $\rm q\bar{q}$ Monte Carlo events, the wrong–sign sample with the background component in the right–sign sample.

Table 1 shows the sample composition of the wrong– and right–sign samples selected from 3.8 million $\rm q\bar{q}$ Monte Carlo events. The numbers of combinatorial background events in the right– and wrong–sign samples are closely similar. The fraction of b baryon events in the wrong–sign sample is due to a combination between a lepton originating from $\Lambda_{\rm b}$ semileptonic decay and a $\Lambda\pi^+$ from fragmentation. Such a combination is suppressed at 99% level in the right–sign sample, because a fragmentation Λ associated with the $\Lambda_{\rm b}$ tends to have a baryon number opposite to that from the $\Lambda_{\rm b}$ cascade decay.

The comparison of the wrong–sign samples in data and Monte Carlo (see Table 2) shows that average energies are compatible. Furthermore, Table 3 shows that

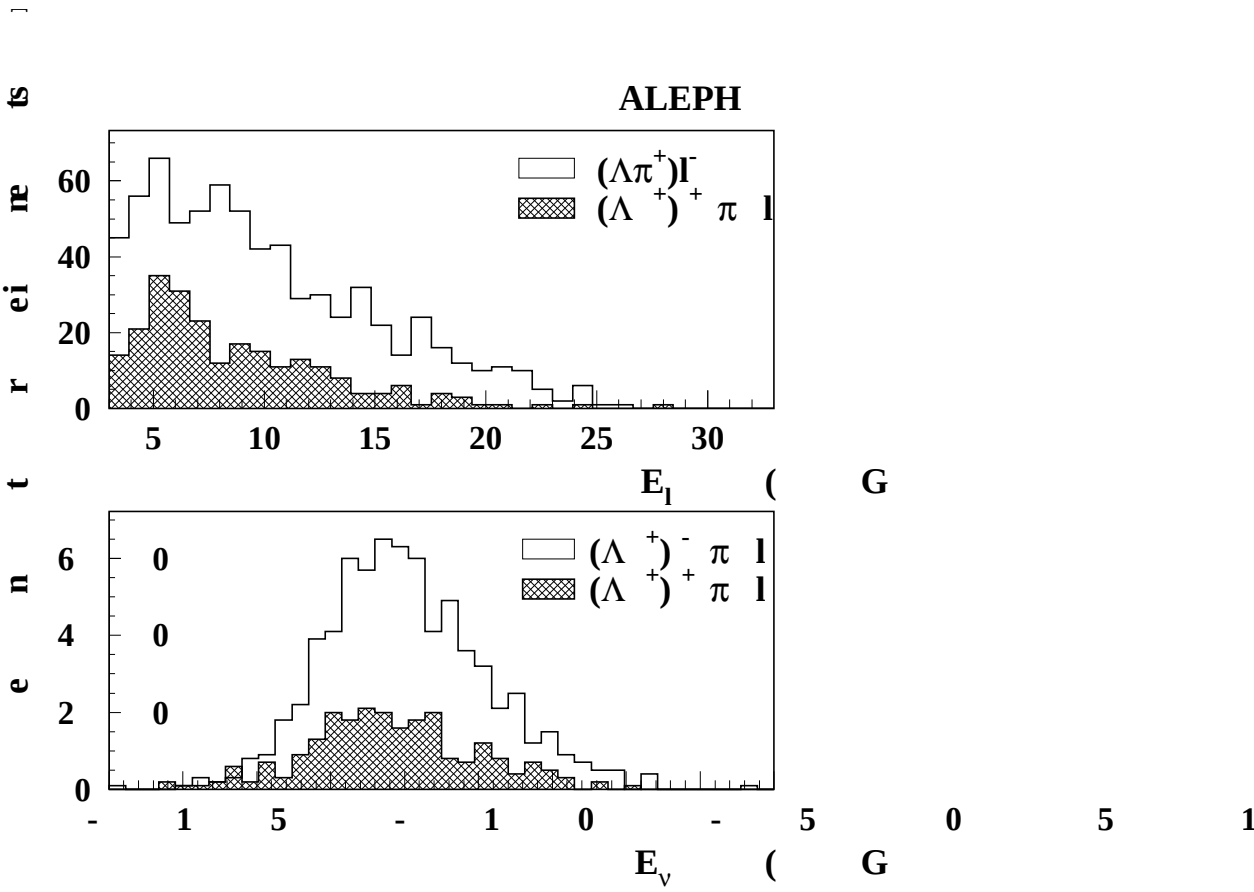

Figure 3: The charged lepton and neutrino energy distributions in the data for the selected right–sign(unhatched histograms) and wrong–sign sample (hatched histograms).

Lepton sources	Right–sign	Wrong–sign
b baryons	475 ± 22	105 ± 10
b mesons	161 ± 13	146 ± 12
c baryons	4 ± 2	15 ± 4
c mesons	45 ± 7	45 ± 7
others (K, γ)	13 ± 4	7 ± 3
fake	36 ± 6	31 ± 6

Table 1: Monte Carlo composition of wrong– and right–sign samples after selection.

the number of background events in the right–sign Monte Carlo sample is well reproduced by the wrong–sign sample and that their corresponding average charged lepton and neutrino energies are also consistent.

The Monte Carlo study shows that the signal events in the wrong–sign sample do not introduce any bias. The average charged lepton energy and the average neutrino energy originating from the Λ_b semileptonic decays are extracted from the

Wrong–sign	$\langle E_\ell \rangle$ (GeV)	$\langle E_\nu \rangle$ (GeV)
Data	8.68 ± 0.28	3.89 ± 0.39
Monte Carlo	8.67 ± 0.23	4.01 ± 0.29

Table 2: Comparison of the numbers of wrong–sign events and their average charged lepton and neutrino energies, in data and in Monte Carlo.

Monte Carlo background	Events	$\langle E_l \rangle$ (GeV)	$\langle E_\nu \rangle$ (GeV)
right–sign	259	8.68 ± 0.26	3.81 ± 0.35
wrong–sign	244	8.50 ± 0.27	3.53 ± 0.32

Table 3: Comparison of the number of background events in the right– and wrong–sign events and their respective average charged lepton and neutrino energies in the Monte Carlo.

right–sign sample using the following background subtraction:

$$\langle E_{\ell,\nu} \rangle = \frac{1}{1 - f_{\rm bck}} \left(\langle E^{\rm RS}_{\ell,\nu} \rangle - f_{\rm bck} \langle E^{\rm WS}_{\ell,\nu} \rangle \right) , \tag{7}$$

where $\langle E^{\rm RS}_{\ell,\nu} \rangle$ and $\langle E^{\rm WS}_{\ell,\nu} \rangle$ are the average charged lepton or neutrino energies measured in the right–sign and the wrong–sign samples respectively; $f_{\rm bck}$ is the background fraction in the right–sign sample, measured in data as

$$f_{\rm bck} = \frac{N_{\rm WS}}{N_{\rm RS}} ,$$

where $N_{\rm WS}$ and $N_{\rm RS}$ are the number of selected wrong–sign and right–sign events respectively. In data, the background fraction is $f_{\rm bck} = 0.33 \pm 0.02$. In the Monte Carlo (Table 1) the background fraction is higher (47%) due mainly to the underestimation of the inclusive $\Lambda_{\rm c} \to \Lambda X$ branching ratio in the ALEPH Monte Carlo. This discrepancy has no influence on the $\Lambda_{\rm b}$ polarization measurement.

5 Results

The y observable is determined from the average charged lepton $\langle E_\ell \rangle$ and neutrino $\langle E_\nu \rangle$ energies for both data and Monte Carlo samples. For the latter unpolarized $\Lambda_{\rm b}$ Monte Carlo samples with and without background are compared. The results are presented in Table 4. The y value from the $\rm q\bar{q}$ Monte Carlo sample is similar to the one extracted from the background–free $\Lambda_{\rm b}$ Monte Carlo signal. This shows the reliability of the background subtraction described in the previous section. The value of $R_y^{\rm data}$ is obtained from the ratio of y values in data and Monte Carlo signal. The result is

$$R_y^{\rm data} = \frac{y_{\rm data}}{y_{\rm MC}(0)} = 1.12 \pm 0.10 ,$$

Sample	$\langle E_\ell \rangle$ (GeV)	$\langle E_\nu \rangle$ (GeV)	y
Data	10.94 ± 0.34	5.59 ± 0.38	1.96 ± 0.17
Monte Carlo $q\bar{q}$	11.07 ± 0.41	6.47 ± 0.51	1.71 ± 0.18
Monte Carlo signal	10.49 ± 0.13	6.00 ± 0.15	1.75 ± 0.06

Table 4: The average charged lepton and neutrino energies of the selected Λ_b semileptonic decays in data and Monte Carlo and their corresponding y values.

where the quoted error is statistical only and takes into account a -20% correlation between the charged lepton energy and the neutrino energy.

The Λ_b polarization is extracted from the comparison between the measured $R_y^{\rm data}$ value above and that expected for different Λ_b polarization values as shown in Fig. 4. The result is

$$\mathcal{P}_{\Lambda_b} = -0.28^{+0.23}_{-0.20}\,.$$

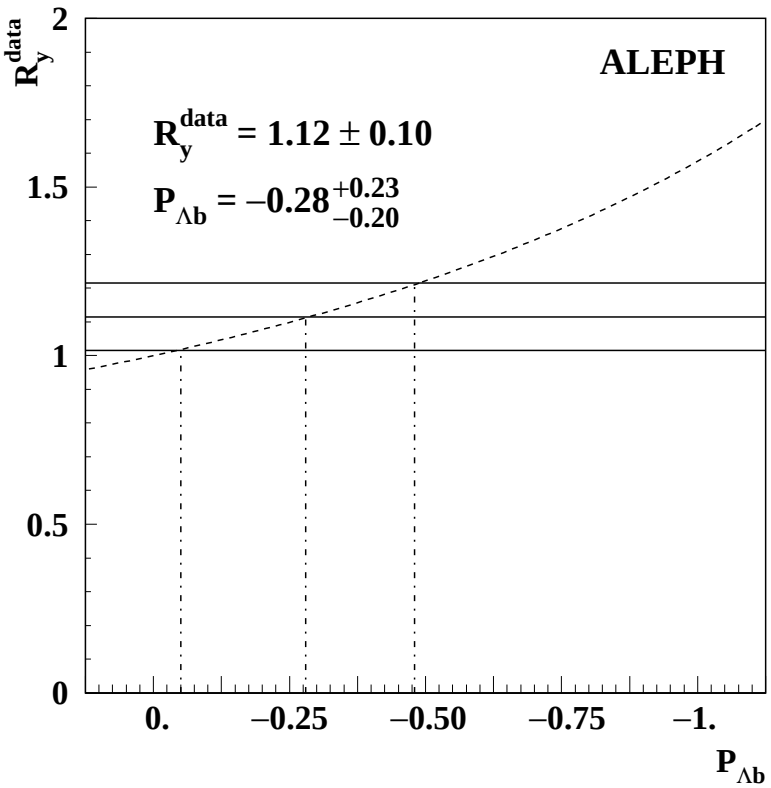

Figure 4: The method used to extract the Λ_b polarization value. Comparison between the measured $R_y^{\rm data}$ value and the theoretical prediction $R_y^{\rm MC}$.

Source		$\sigma_{\mathcal{P}_{\Lambda_b}}$
Missing energy	± 100 MeV	± 0.04
Lepton energy	± 80 MeV	± 0.02
R_y calibration	± 0.025	$^{+0.06}_{-0.05}$
Background fraction $f_{\rm bck}$	$33 \pm 7\%$	$^{+0.03}_{-0.02}$
Reconstruction and acceptance		± 0.02
Λ_c^+ polarization		± 0.01
Theory (m_c^2/m_{b^2}, QCD)		± 0.01
Total		$^{+0.08}_{-0.07}$

Table 5: Systematic uncertainties

6 Systematic uncertainties

Several sources of systematic uncertainties are considered. Their contributions to the total systematic error on the Λ_b polarization measurement are summarized in Table 5.

6.1 Charged lepton and neutrino energy measurements

The Λ_b polarization is determined from $R_y^{\rm data}$ which relies on a comparison of the average charged lepton energy and the average neutrino energy measurements in the data with those in the Monte Carlo. It is therefore crucial to have a good agreement between data and Monte Carlo for the charged lepton energy and the missing neutrino energy measurements. For this purpose, dedicated hadronic events control samples are used. Since the selected $(\Lambda\pi^+)l$ sample has a b purity of 90%, control samples enriched in $b\bar{b}$ events are considered.

6.1.1 Charged lepton energy

The agreement of the charged lepton energy measurement in Monte Carlo and data is studied using two control samples selected from hadronic events: *i*) a sample **A** of inclusive lepton events with $b\bar{b}$ lifetime tag, selected as described in Ref. [16] (b purity $\sim 96\%$), and *ii*) a sample **B** of inclusive lepton events with a lepton transverse momentum $p_T > 1$ GeV/c (b purity $\sim 90\%$). Table 6 compares the average lepton energy in Monte Carlo and data from the two control samples. They agree within 80 MeV. The shapes of the lepton momentum spectra in data and Monte Carlo for the two control samples agree also very well.

Since many potential sources (e.g. hadronization, mass of charmed hadron, ...) of this small disagreement cancel in the ratio with the neutrino energy, the 80 MeV difference is to be taken as a conservative upper uncertainty on y. Varying the average charged lepton energy within ± 80 MeV leads to a Λ_b polarization error of ± 0.02.

	$\langle E_\ell \rangle$ (GeV) sample **A**	$\langle E_\ell \rangle$ (GeV) sample **B**
Data	8.34 ± 0.02	10.26 ± 0.03
Monte Carlo ($q\bar{q}$)	8.26 ± 0.03	10.27 ± 0.05

Table 6: The average charged lepton energy in the two inclusive lepton control samples **A** and **B**.

	$\langle E_{miss} \rangle$ (GeV) sample **A**	$\langle E_{miss} \rangle$ (GeV) sample **C**
Data	6.10 ± 0.03	1.03 ± 0.04
Monte Carlo ($q\bar{q}$)	6.16 ± 0.03	1.10 ± 0.04

Table 7: The average missing energy in two control samples (with and without lepton) for data and $q\bar{q}$ Monte Carlo.

6.1.2 Neutrino energy

To study how well the missing energy measurement in the Monte Carlo reproduces that in the data, two control samples selected in hadronic events are used: *i*) the sample **A** used above and *ii*) a sample **C** of $b\bar{b}$ lifetime–tagged events without leptons (b purity $\sim 90\%$). The two control samples are independent by construction. They allow for an estimation of any bias in the missing energy measurement due to imperfections in the Monte Carlo simulation.

Table 7 shows the average missing energy in the two control samples for data and Monte Carlo. In the two samples, the data and Monte Carlo agree to within 70 MeV. In the lepton sample, which corresponds to the analysis sample, the agreement is at the 60 MeV level.

In order to study the influence of particle identification on the missing energy, events containing an identified proton, $K^{\pm}$, Λ or K^0_S are selected in the tagged or the anti-tagged lepton hemisphere. The differences between the average missing energies in data and Monte Carlo are consistent with those observed in the inclusive samples.

Varying the average missing energy in the Λ_b semileptonic decay Monte Carlo sample within ± 100 MeV leads to a systematic error of ± 0.04 on the measured Λ_b polarization.

6.1.3 R_y calibration

The lepton inclusive sample **B** is taken as a calibration sample for R_y. As b mesons ($\sim 90\%$ of b hadrons) are unpolarized and the measured Λ_b polarization value is rather low, the R_y of this sample should be close to 1. The value obtained is 1.05 ± 0.01 showing a discrepancy between data and Monte Carlo for high p_T leptons. To take this disagreement into account, the central value of the R_y^{data} in the Λ_b polarization analysis is shifted by -0.025 and a systematic error of ± 0.025 is associated to R_y. This conservative procedure overestimates the systematic error as includes the neutrino and lepton energy uncertainties, already counted. The Λ_b

polarization value is shifted by $+0.045$ and the induced error is ± 0.05.

6.2 Background fraction

The fraction of background events enters the determination of the average charged lepton and neutrino energies (Eq. 7). The difference between the number of wrong–sign events in the data and the Monte Carlo is of the order of 20%. This corresponds to an error of $\pm 7\%$ with respect to the right–sign sample, and translates to a systematic uncertainty of $^{+0.03}_{-0.02}$ on the Λ_b polarization.

6.3 Corrections due to reconstruction and selection cuts

The analytical curve that reproduces the variation of R_y as a function of the Λ_b polarization is used to extract the Λ_b polarization. A correction is introduced to take into account the effects of the reconstruction and the selection cuts on R_y (see Section 3.3). Varying this correction within its error leads to an uncertainty on the Λ_b polarization of ± 0.02.

6.4 Λ_c^+ polarization

The Λ_c^+ polarization in Λ_b events can affect the results of the present analysis. Cuts on the Λ momentum (at 3 GeV/c) and on the angle between the Λ and the charged lepton (45°) can introduce biases due to the topological correlation between the spin states of the Λ_b and the Λ_c^+. Since in the ALEPH Monte Carlo the Λ_c^+ and Λ_b baryons are unpolarized, a dedicated Monte Carlo is used to produce the decay chain $\Lambda_b \to \Lambda_c^+ \ell^- \bar{\nu}_\ell$, $\Lambda_c^+ \to \Lambda\pi^+$ where both Λ_b and Λ_c^+ are polarized. The Λ_c^+ events are weighted using the function

$$W(\cos\theta_\Lambda) = 1 + \alpha_{\Lambda_c} \mathcal{P}_{\Lambda_c} \cos\theta_\Lambda \,, \tag{8}$$

where θ_Λ is the angle between the Λ and Λ_c^+ momenta in the Λ_c^+ rest system, $\mathcal{P}_{\Lambda_c}$ is the Λ_c^+ polarization and $\alpha_{\Lambda_c} \simeq -1$ as measured by CLEO and ARGUS [17].

The branching ratio of $\Lambda_c \to \Lambda\pi^+$ is overestimated by a factor 3 in order to account for the non-zero analyzing power of the other channels. Varying the Λ_c^+ polarization from 0 to -1 leads to a variation of the Λ_b polarization of 0.02. Half this value is quoted as a systematic error and the central value is shifted by $+0.01$.

6.5 Theoretical errors

Theoretical errors arise from three sources.

- The poorly known ratio of the charm and beauty masses enters the theoretical determination of y. Varying m_c^2/m_b^2 between 0.06 and 0.13 leads to a negligible change of Λ_b polarization.

- Non–perturbative corrections appear only to $\mathcal{O}(\Lambda_{\rm QCD}/m_{\rm b})^2$ [11](a quantity of order 1%) and are neglected.
- Perturbative QCD corrections turn a small percentage of the $\Lambda_{\rm b}$ events into four-body decays, due to the presence of gluons which produce a small loss in sensitivity. These corrections are calculated in Ref. [18]. Varying α_s between 0.10 and 0.30 leads to an uncertainty on the $\Lambda_{\rm b}$ polarization of ± 0.01.

Combining the systematic errors from the different sources in quadrature leads to a total systematic error of $^{+0.08}_{-0.07}$. The final $\Lambda_{\rm b}$ polarization value, including the corrections and the total systematic error, is

$$\mathcal{P}_{\Lambda_{\rm b}} = -0.23^{+0.24}_{-0.20}({\rm stat.})^{+0.08}_{-0.07}({\rm syst.}).$$

7 Conclusions

The $\Lambda_{\rm b}$ polarization has been measured using semileptonic decays selected from a data sample of approximately 3 million hadronic Z decays collected with the ALEPH detector between 1991 and 1994. The $\Lambda_{\rm b}$ semileptonic decay events were selected using the charge correlation between the $(\Lambda\pi^+)$ system and a lepton in the same hemisphere of a hadronic Z decay. The final sample consists of 462 ± 31 $\Lambda_{\rm b}$ candidates. The ratio between the average charged lepton energy and average neutrino energy of this sample is sensitive to the $\Lambda_{\rm b}$ polarization. This ratio was normalized to that extracted from an unpolarized sample of $\Lambda_{\rm b}$ semileptonic Monte Carlo events. From this ratio, the $\Lambda_{\rm b}$ polarization is measured to be

$$\mathcal{P}_{\Lambda_{\rm b}} = -0.23^{+0.24}_{-0.20}({\rm stat.})^{+0.08}_{-0.07}({\rm syst.})\,.$$

This result corresponds to a loss of $(76\pm26)\%$ of the initial b quark polarization in the process of fragmentation down to $\Lambda_{\rm b}$. This surprisingly small polarization value is two standard deviation from expectation (-0.69 ± 0.06). Barring the existence of V + A currents, which are not observed in the quark sector, this result may point to depolarizing mechanisms occurring during hadronization which are yet to be understood.

Acknowledgements

We whish to thank our colleagues from the accelerator divisions for the successful operation of LEP. We are indebted to the engineers and technicians at CERN and our home institutes for their contribution to the good performance of ALEPH. Those of us from non member countries thank CERN for its hospitality.

References

[1] J.G. Körner, A. Pilaftsis and M. Tung, Z. Phys. **C 63** (1994) 575

[2] F.E. Close, J.G. Körner , R.J.N. Phillips and D.J. Summers, J. Phys. **G 18** (1992) 1716.

[3] A.F. Falk and M.E. Peskin, Phys. Rev. **D 49** (1994) 3320.

[4] D. Buskulic *et al.*, (ALEPH Collab.), Phys. Lett. **B 359** (1995) 236.

[5] DELPHI Collab., contributed paper to EPS-HEP 1995 conference, Brussels, 27th July-2nd August 1995, Ref. EPS0565.

[6] M. Gronau, in *B decays* 2nd edition, ed. by S. Stone, p. 644, World Scientific, Singapore (1994).

[7] D. Decamp *et al.*, (ALEPH Collab.), Nucl. Instrum. and Method. **A294** (1990) 121;

D. Buskulic *et al.*, (ALEPH Collab.), Nucl. Instrum. and Method. **A346** (1994) 461.

[8] D. Buskulic *et al.*, (ALEPH Collab.), Nucl. Instrum. and Method. **A360** (1995) 481.

[9] G. Bonvicini and L. Randall, Phys. Rev. Lett. **73** (1994) 392.

[10] J.G. Körner and M. Krämer, Phys. Lett. **B 275** (1992) 495; T. Mannel and G.A. Schuler, Phys. Lett. **B 279** (1992) 194; G. Altarelli and B. Mele, Phys. Lett. **B 299** (1993) 345; J.F. Amundson, J.L. Rosner, M. Worah and M.B. Wise, Phys. Rev. **D 47** (1993) 1260.

[11] J. Chay, H. Georgi and B. Grinstein, Phys. Lett. **B 247** (1990) 399; A.V. Manohar and M.B. Wise, Phys. Rev. **D 49** (1994) 1310.

[12] D. Decamp *et al.*, (ALEPH Collab.), Z. Phys. **C 53** (1992) 1.

[13] D. Decamp *et al.*, (ALEPH Collab.), Phys. Lett. **B 257** (1991) 492;

[14] T. Sjostrand, Comp. Phys. Com. **82** (1994) 74. Throughout this analysis, a modified version of the JETSET 7.3 program was used to generate both $Z \to q\bar{q}$ events and Λ_b semileptonic decays. The generated Monte Carlo events are processed through a full simulation of the performance characteristics of the ALEPH detector.

[15] D. Buskulic *et al.*, (ALEPH Collab.), Phys. Lett. **B 322** (1994) 275.

[16] D. Buskulic *et al.*, (ALEPH Collab.), Phys. Lett. **B 298** (1993) 479.

[17] P. Avery *et al.*, (CLEO Collab.), Phys. Rev. Lett. **65** (1990) 2842; H. Albrecht *et al.*, (ARGUS Collab.), Phys. Lett. **B 274** (1992) 239.

[18] A. Czarnecki, M. Jezabek, J.G. Körner , and J. Kuhn, TTP 93-332, MZ-TH/**93-35**, hep-ph 9312249.